## Mechanical Response of Al Matrix Syntactic Foams Produced by Pressure Infiltration Casting


L.P. Zhang and Y.Y. Zhao



*Journal of Composite Materials* 2007; 41; 2105
DOI: 10.1177/0021998307074132

# Mechanical Response of Al Matrix Syntactic Foams Produced by Pressure Infiltration Casting

L. P. ZHANG AND Y. Y. ZHAO*
*Department of Engineering, The University of Liverpool, Liverpool, L69 3GH, UK*

**ABSTRACT:** Aluminum matrix syntactic foams with low-cost porous ceramic spheres of diameters between 0.25 and 4 mm have been manufactured by pressure infiltration casting. These syntactic foams were homogeneous in structure and had densities as low as half of the density of the Al matrix. The mechanical response of the four types of syntactic foams with different sphere sizes and densities under static and dynamic conditions have been investigated. The plateau strength and thus the amount of energy absorption of the syntactic foam are largely determined by the volume fraction of Al and to a lesser extent by the mechanical properties of the ceramic spheres in the foam. Compared with the Al foams with similar Al volume fractions, the syntactic foams had better energy absorption capacity, especially under impact conditions.

**KEY WORDS:** liquid infiltration, aluminum, foams, compression test, impact test.

## INTRODUCTION

DEVELOPMENT OF MATERIALS for the protection of human bodies, buildings, vehicles and machineries against impact and blast is a constant challenge facing the materials community. Porous or foamed materials are good energy absorbers because a large amount of impact energy can be absorbed by their sacrificial collapse through buckling, plastic yielding, or brittle crushing of the cell walls [1–4]. The capacity of a porous material in energy absorption can largely be characterized by its plateau strength and porosity. Plateau strength is the stress around which the porous material undergoes large deformation; it is an important parameter because it must not exceed the stress the object under protection can withstand. The porosity of the materials determines the

*Author to whom correspondence should be addressed. E-mail: y.y.zhao@liv.ac.uk
Figure 6 appears in color online: http://jcm.sagepub.com/



0021-9983/07/17 2105–13 $10.00/0 DOI: 10.1177/0021998307074132

maximum deformation achievable without causing damage to the subject under protection. The maximum energy absorbed by per unit volume of the porous material before the densification can be approximately calculated as the product of the plateau strength and porosity. For a given material, however, the plateau strength is also dependent on the porosity. The higher the porosity, the lower the plateau strength. Although the energy absorbing capacity can be modulated to some extent by varying porosity, the maximum energy a porous material can absorb is more or less determined by the type and composition of the matrix material.

There are currently a wide range of porous materials available. Polymer foams have low plateau strength and are suitable for protecting human bodies and delicate objects from relatively low velocity and low energy impacts. Because of their relatively low strength, low stiffness, low temperature capability, high flammability and susceptibility to degradation in many environments, polymer foams cannot be used in more demanding structural applications. Porous ceramics alone are not good energy absorbers. Although ceramics have high strengths, they are inherently brittle. Ceramics subject to impact are immediately shattered and absorb little amounts of energy. Metal foams have recently attracted an increasing level of interest in both academia and industry because of their good combinations of strength, stiffness, ductility, temperature capability, and durability. Metal foams have much higher plateau strength than polymer based foams and are therefore suitable for protections against impacts of much higher energies. They can be used as lightweight panels for buildings against buckling and impact, crash-boxes, and passenger-door inserts in cars to improve the crashworthiness and passenger safety, and protective skins of military vehicles against explosives and projectiles.

Syntactic foam incorporates hollow or porous ceramic spheres in a polymer or metal matrix to produce high specific stiffness and strength. Whereas polymer matrix syntactic foam has been available commercially for some time, metal matrix syntactic foam has not been manufactured and studied until very recently. Hartmann et al. [5] produced a series of Mg alloy matrix syntactic foams with densities varying between 0.9 and 1.8 $g/cm^3$. They investigated the effect of foam density on specific stiffness and strength and concluded that both the matrix and the spheres contribute to the overall strength of the syntactic foam. Kiser et al. [6] studied the mechanical response of Al matrix syntactic foams reinforced with hollow $Al_2O_3$ spheres under uniaxial and constrained die compression loading conditions. Their work showed that the hollow spheres, especially those with thin walls, easily cracked during the fabrication and compression tests. Under uniaxial compression conditions the failure initiated at relatively small strains (1–2%) and the material exhibited poor energy absorption, whereas under constrained die compression conditions the material exhibited high energy absorption capacity (about 60–70 $J/cm^3$). The hollow spheres were shown to have a strong reinforcing effect rather than providing porosity. Up to date, the metal matrix syntactic foams studied have been limited to those reinforced with the hollow ceramic spheres. Very little research has been reported on the metal matrix syntactic foams reinforced with porous ceramic spheres.

In this article, Al matrix syntactic foams reinforced with several types of porous ceramic spheres are produced by the pressure infiltration casting method; the mechanical response and energy absorption of the as-manufactured Al matrix syntactic foams under static and dynamic conditions are investigated; and the energy absorption capacity of the syntactic foams is compared with the open cell Al foams produced by the pressure infiltration casting method [7].

## EXPERIMENTAL

### Raw Materials

The raw materials used in this study were commercially pure Al and four types of porous ceramic spheres. Sphere Type A, supplied by Envirospheres Pty Ltd. in Australia, has a composition of 60 wt% $SiO_2$ and 40 wt% $Al_2O_3$. Types B, C, and D, supplied by Omega Minerals Ltd. in Germany, have a similar composition of 60 wt% $SiO_2$, 15 wt% $Al_2O_3$, 15 wt% CaO and 10 wt% $Na_2O$, but different sphere sizes. Figure 1 shows an SEM micrograph of a mixture of the four types of spheres, which were coated with gold by an S-150 sputter coater. All the four types of spheres have a similar morphology. The porous spheres are nearly spherical and have a rough surface. Table 1 lists the supplier specifications of the four types of spheres, including size range, effective density, compressive strength, and the estimated average porosity. Type A has the smallest sphere sizes, a medium effective density and a relatively high compressive strength of 45 MPa. Types B, C, and D have a similar compressive strength within 14–18 MPa but different size ranges and effective densities. Larger spheres have lower densities.

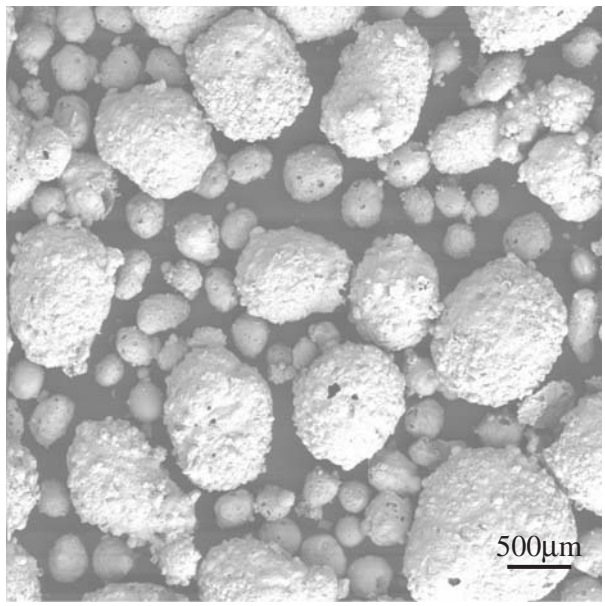


***Figure 1.*** *SEM micrograph of ceramic spheres.*

***Table 1. Properties of ceramic spheres used in the experiments.***

| Sphere type | A | B | C | D |
|---|---|---|---|---|
| Size range (mm) | 0.25–0.5 | 0.5–1 | 1–2 | 2–4 |
| Effective density, $\rho_s$ (g/cm$^3$) | 0.75 | 0.95 | 0.8 | 0.65 |
| Compressive strength (MPa) | 45 | 14–16 | 16–18 | 14–18 |
| Average porosity, $\varphi_s$ | 0.76 | 0.66 | 0.71 | 0.77 |

The average porosity of each type of ceramic spheres was estimated by

$$\varphi_s = \left(1 - \frac{\rho_s}{\rho_o}\right) \tag{1}$$

where $\rho_s$ is the effective density of the spheres and $\rho_o$ is the density of the solid part of the spheres, i.e., the density of the solid ceramic. Because the density of the solid part of the spheres was difficult to be determined by experimental methods, it was estimated from the composition. Given that the densities of $SiO_2$, $Al_2O_3$, CaO, and $Na_2O$ are 2.65, 3.97, 3.34, and 2.27 g/cm$^3$, respectively [8], the density of the solid part of the Type A spheres was calculated to be $\rho_o = 3.05$ g/cm$^3$ and that of the Types B, C, and D spheres was calculated to be $\rho_o = 2.83$ g/cm$^3$.

## Sample Preparation

Four types of Al matrix syntactic foams, corresponding to Types A, B, C, and D ceramic spheres and designated as Foams I, II, III, and IV, respectively, were produced by pressure infiltration casting. In the fabrication of a syntactic foam sample, a steel tube with a diameter of 21 mm and a height of 60 mm, sealed by a circular steel disk at the bottom, was first partly filled with the ceramic spheres. An Al block was then placed on the top of the spheres. Another circular steel disk, which was slightly smaller than the internal diameter of the tube, was placed above the Al block. The volume ratio of the Al and ceramic spheres was maintained at 1:2, at which the Al was slightly more than the amount needed to ensure full infiltration. The assembly was placed in an electric furnace, heated up and maintained at 730°C for 30 min to ensure that the Al block was fully molten. The assembly was then removed from the furnace and placed in a hydraulic press where a ram pushed the top steel disk down until the pressure reached about 4 MPa so that the molten aluminum infiltrated the interstices of the ceramic spheres. After the Al fully solidified the sample was pushed out of the steel tube. The steel disks and the excessive Al layer at the top of the sample were removed. The resultant cylindrical syntactic foam sample was machined and ground for subsequent analysis. The dimensions of the samples for mechanical tests were 20 mm in diameter and about 30 mm in length.

## Sample Characterization

The density of each syntactic foam sample was measured by the Archimedes method. The porosity of the sample was estimated from its density and the porosity of the ceramic spheres used in fabricating the sample. For a syntactic foam sample, the densities of the sample, the Al matrix, and the ceramic spheres, $\rho_f$, $\rho_{Al}$ and $\rho_s$ respectively, are related by the rule of mixture:

$$\rho_f = f_{Al}\rho_{Al} + (1 - f_{Al})\rho_s \tag{2}$$

where $f_{Al}$ is the volume fraction of the Al matrix in the foam sample, which can therefore be determined by:

$$f_{Al} = \frac{\rho_f - \rho_s}{\rho_{Al} - \rho_s}. \tag{3}$$

The porosity of the foam is therefore:

$$\varphi_f = (1 - f_{\mathrm{Al}})\varphi_s = \frac{\rho_{\mathrm{Al}} - \rho_f}{\rho_{\mathrm{Al}} - \rho_s}\left(1 - \frac{\rho_s}{\rho_o}\right). \tag{4}$$

The microstructure of the syntactic foam samples was examined by optical and scanning electron microscopy. The static compression tests of the samples were carried out on an Instron 4505 materials testing machine at a crosshead speed of $1.67 \times 10^{-5}$ m/s. The dynamic impact tests were conducted on an ESH testing system at a hammer speed of 2 m/s. At least two samples were tested under each condition to verify the repeatability. The mechanical response of the loose compact of each type of ceramic spheres under the compressive condition was also studied. A small volume of each type of spheres was put into a cylindrical tube and compressed on the Instron 4505 at a crosshead speed of $1.67 \times 10^{-5}$ m/s under the constrained die compression condition.

## RESULTS

### Structural Characteristics of Syntactic Foams

Figure 2 shows the typical cross-sectional micrographs of the syntactic foams. In each sample, the ceramic spheres are uniformly distributed in the Al matrix. The ceramic spheres are not entirely hollow but contain many small pores. Sphere A in Foam I contains homogeneously dispersed air bubbles with similar sizes. Spheres B, C, and D in Foams II, III, and IV, respectively, have relatively thin shells and contain irregular pores with

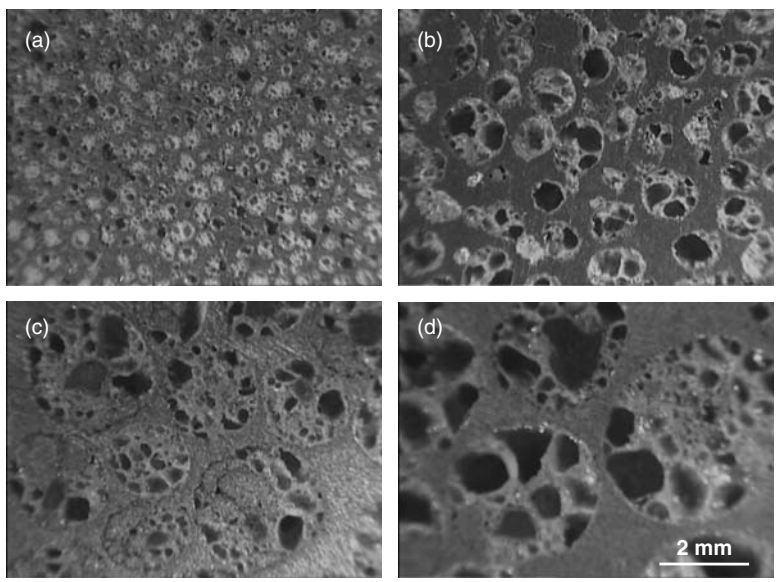


***Figure 2.*** *Optical cross-sectional micrographs of the syntactic foam samples: (a) Foam I; (b) Foam II; (c) Foam III; (d) Foam IV.*

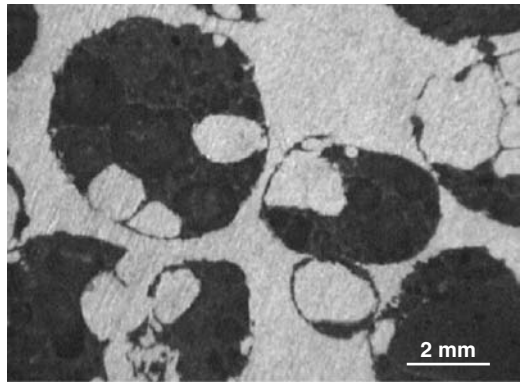


***Figure 3.*** *Micrograph of Foam IV showing the region where some porous spheres are partly infiltrated with Al.*

***Table 2. Density, volume fraction of Al and porosity of the syntactic foams.***

| Foam | I | II | III | IV |
|---|---|---|---|---|
| Foam density, $\rho_f$ (g/cm$^3$) | 1.38 | 1.58 | 1.83 | 1.88 |
| Volume fraction of Al, $f_{Al}$ | 0.32 | 0.36 | 0.54 | 0.60 |
| Foam porosity, $\varphi_f$ | 0.51 | 0.44 | 0.34 | 0.31 |

thick walls. The shells of spheres C and D are particularly weak. Some shells are not water-tight; consequently some spheres are partly or fully penetrated by the Al melt during the infiltration casting process, as shown in Figure 3.

Table 2 lists the densities, volume fractions of Al and porosities of the syntactic foams I, II, III, and IV. The volume fractions of Al matrix, $f_{\mathrm{Al}}$, and the porosities, $\varphi_f$, of the syntactic foams were estimated by Equations (3) and (4) based on the measured values of foam densities. It is shown that with increasing size of the reinforcing ceramic spheres the density and volume fraction of Al of the syntactic foams increased while the porosity of the foams decreased. The volume fraction of Al in a syntactic foam is expected to be close to the interspherical porosity in the ceramic sphere compact, which is normally around one third. Due to the penetration of Al into some weak ceramic spheres during infiltration casting, Foams III and IV have particularly high volume fractions of Al. However, the volume fractions of solid ceramic in the syntactic foams, $(1–f_{\mathrm{Al}}–\varphi_f)$, do not vary greatly and fall within 0.12–0.19.

## Behavior of Ceramic Sphere Compacts under Static Compression

The stress–strain curves of the compacts of ceramic spheres A, B, C, and D under static compression are shown in Figure 4. The compacts as a whole had no discernible elastic stages and underwent plastic deformation throughout the compression. In the initial stage of the compression of a compact, the ceramic spheres were first rearranged and the interspherical porosity was reduced. Increasing stress further led to gradual crushing of some spheres, largely because of highly localized stress concentrations. The stress increased steadily with increasing strain due to continual densification. The ceramic spheres

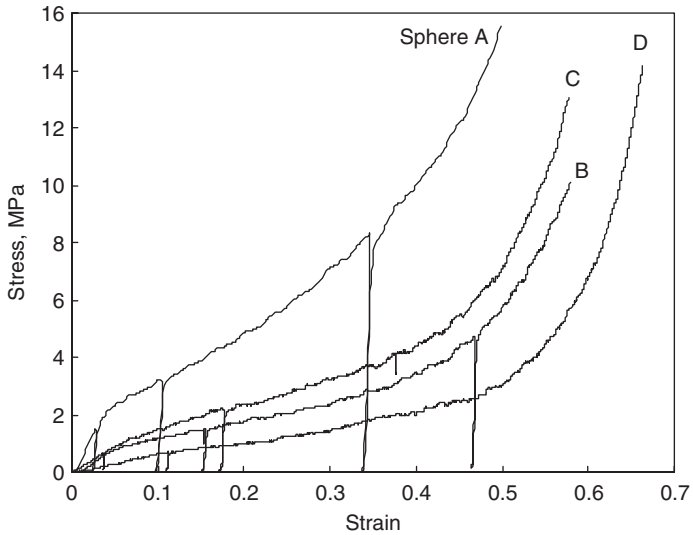


***Figure 4.*** *Stress–strain curves of the compacts of the four ceramic spheres under static compression.*

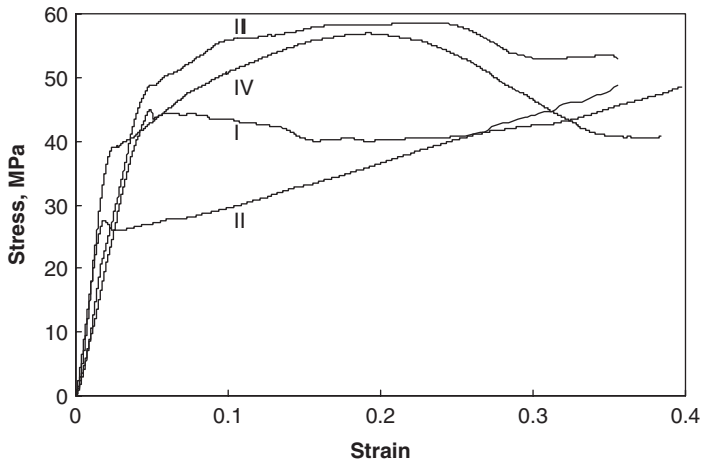


***Figure 5.*** *Typical stress–strain curves of syntactic foams in uniaxial static compression.*

collectively had a much lower compressive strength than that of the individual spheres specified by the suppliers. The compressive strengths of the compacts were dependent not only upon the compressive strength of the individual spheres but also upon the sphere size. At any fixed strain, the order of compact stress from high to low is: A, C, B, and D. The compact of sphere A has a much higher stress than the others.

## Behavior of Syntactic Foams under Static Compression

The syntactic foam samples manufactured under the same conditions showed reasonably repeatable behavior under static uniaxial compression tests. Figure 5 shows

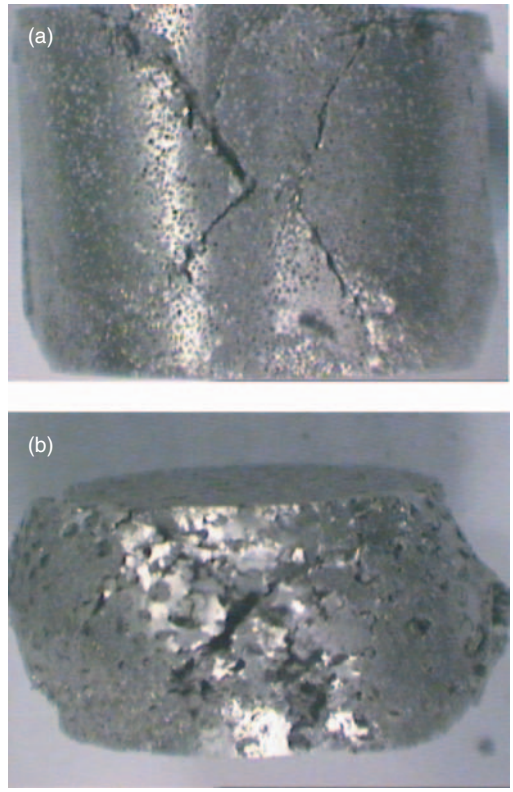


***Figure 6.*** *Macrographs showing the cracks appeared in the samples during static compression (a) Foam I at a strain of 0.25 and (b) Foam III at a strain of 0.35.*

the representative stress–strain curves for the four types of syntactic foams under static compression. All four curves have a linear elastic part, from which the moduli of elasticity of Foams I, II, III, and IV were determined to be approximately 1030, 1710, 1120, and 1780 MPa, respectively. The plastic deformation began at strains of roughly 0.05, 0.02, 0.05 and 0.03 and at corresponding stresses of roughly 45, 28, 49 and 39 MPa for Foams I, II, III, and IV, respectively. Subsequently, the foams underwent large plastic deformation under relatively narrow ranges of stresses. Foams I, III, and IV showed rapid stress drops at strains of around 0.15, 0.25, and 0.30, respectively. These stress drops corresponded to the appearance of cracks in the samples. Figure 6 shows the photographs of the Foam I and Foam III samples during compression when cracks appeared. The cracks are X shaped and at 45° to the axial direction, typical of shear fracture.

## Behavior of Syntactic Foams under Impact

Figure 7 shows typical stress–strain curves for Foams I–IV under the impact condition. The impacting hammer experienced strong vertical vibrations when it hit the foam samples. As a consequence, the curves show great oscillations at low strains. With increasing strain, the oscillations are gradually dampened down. On the average, however,

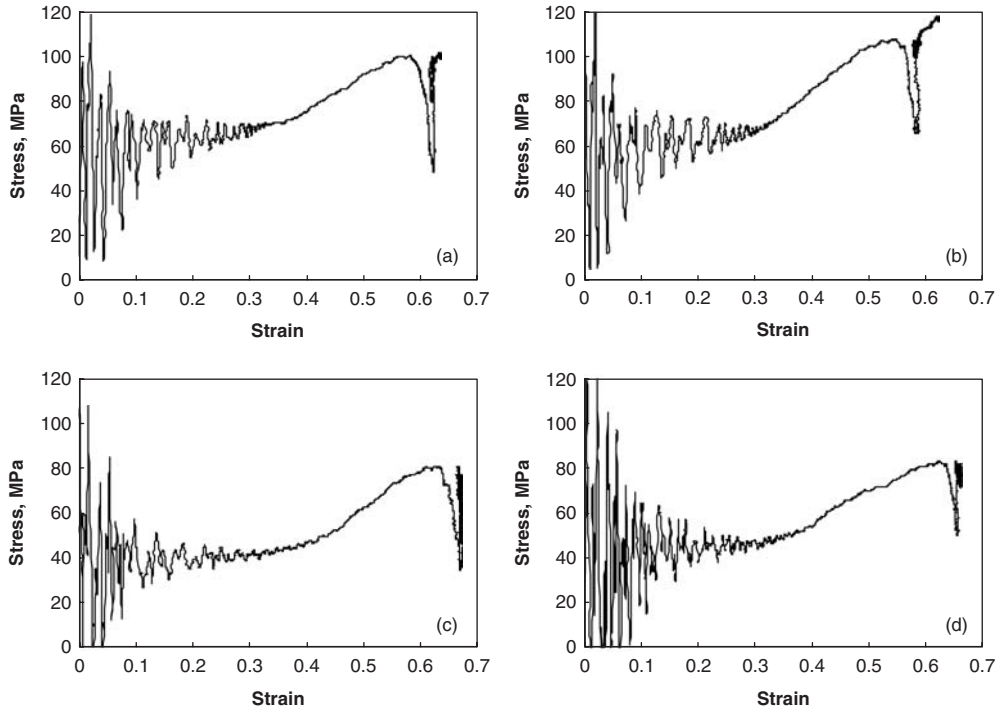


***Figure 7.*** *Typical stress–strain curves of the four syntactic foams under impact: (a) Foam I; (b) Foam II; (c) Foam III; (d) Foam IV.*

the central stress of the oscillations for each sample was nearly constant before densification started at a strain between 0.3 and 0.4. In other words, there appear to be a distinctive plateau stress before densification for each sample. Averaging the stresses over strains below 0.3 gives the plateau stresses of 62, 62, 41, and 44 MPa for Foams I, II, III, and IV, respectively. At strains above 0.3–0.4, the stresses increased steadily until the hammer stopped. The onset of stress increase was related to the densification process.

## DISCUSSION

### Deformation and Fracture

The onset of severe plastic deformation (yielding) of the syntactic foams is determined by the compressive strength and volume fraction of the ceramic spheres, because large amount of plastic deformation results from the gradual collapse of the ceramic spheres. As a simple illustration, the relationship between the yielding strength of the syntactic foam and the properties of the ceramic spheres can be explained by the rule of mixture. Let us assume that the stress share in the network of ceramic spheres is proportional to its volume fraction in the syntactic foam. Given the nominal compressive strengths of Sphere Types A, B, C, and D of 45, 15, 17, and 16 MPa (Table 1), and their volume fractions in Foams I, II, III, and IV of 0.68, 0.64, 0.46,

and 0.40 (Table 2), the yielding strengths of the foams are estimated to be 66, 23, 37, and 40 MPa, respectively. The estimated values of the yielding strength are different from the measured ones, which are 45, 28, 49, and 39 MPa for Foams I, II, III, and IV, respectively. The difference is partly due to the crude nature of the rule of mixture and partly due to the unreliable compressive strength values of the ceramic spheres provided by the suppliers. Figure 4 shows that the ceramic sphere compact has a much lower compressive strength than that of the individual spheres specified by the suppliers. It also shows that at any strain the decreasing order of compressive stress is: Spheres A, C, B, and D. The compressive strengths of Spheres B, C, and D are clearly different, instead of having a similar nominal value as indicated by the supplier.

During compression, the majority of the syntactic foams cracked in the late stage of plastic deformation. The characteristic shear fracture was a consequence of the unique structure of the Al matrix syntactic foam. The syntactic foam can be seen as two intermingled networks of Al and ceramic spheres. The Al network is a continuous reticulation of dense struts. The ceramic network is mainly composed of touching ceramic spheres, provided they are not disturbed significantly during the pressure infiltration casting process. Some individual ceramic spheres and clusters of several ceramic spheres may be completed imbedded in the Al matrix, similar to that in a conventional metal matrix composite. In any case, the ceramic network alone cannot withstand any shear or tensile loading. The shear stresses within the syntactic foam are completely borne by the Al network. The compressive stresses, on the other hand, are shared between the Al and ceramic networks. The mode of failure of the syntactic foam depends on which of the compressive and shear limits is reached first. If the compressive component of the stresses exceeds the compressive strength of the ceramic spheres, the spheres collapse successively and the foam as a whole undergoes plastic deformation. If the shear component of the stresses (the maximum of which is at an angle of 45° to the loading direction) exceeds the shear strength of the Al network, the syntactic foam fractures. Lower volume fraction of Al in the syntactic foam seems to lead to earlier fracture failure. In this study, however, a clear pattern in the transition from compressive failure to shear failure has not been identified. The random occurrences of cracking may be linked to internal defects in the syntactic foams, which can result from non-uniform structures of the ceramic spheres and incomplete melt infiltration at certain locations.

## Energy Absorption

The two most important parameters of a porous material for energy absorption purposes are the plateau strength and the densification strain, which is the maximum strain a stress equal to the plateau strength can achieve. In an ideal situation where the porous material undergoes plastic deformation at a stress equal to the plateau strength until all the pores are closed, the densification strain is exactly equal to the porosity of the porous material. In practice, the strength of the porous material increases when the porosity is reduced to a certain level; it is often impossible to close all the pores. As a consequence, densification can start at a strain significantly lower than the porosity. In the static compression tests, the Al matrix syntactic foams often cracked well before the strain reached the porosity level. In the impact tests, the densification strains of the syntactic foams were within the range of 0.3–0.4, not very

***Table 3. Plateau strength and specific energy absorbed at a strain of 0.3 for the syntactic foams under static compression and impact conditions.***

| Foam | | I | II | III | IV |
|---|---|---|---|---|---|
| Volume fraction of Al, $f_{Al}$ | | 0.32 | 0.36 | 0.54 | 0.60 |
| Ceramic sphere size (mm) | | 0.25–0.5 | 0.5–1 | 1–2 | 2–4 |
| Plateau strength (MPa) | Static | 41.7 | 33.3 | 55.6 | 51.4 |
| | Impact | 62.3 | 62.1 | 40.6 | 44.1 |
| Energy absorbed (J/cm$^3$) | Static | 12.1 | 9.8 | 15.4 | 14.7 |
| | Impact | 18.4 | 18.2 | 12.0 | 13.1 |

sensitive to the porosity. In the following analysis, only the energy absorption behavior below a strain of 0.3 is considered.

Table 3 lists the values of the plateau strength and the specific energy absorbed at a strain of 0.3 for the syntactic foams under static compression and impact conditions. The specific energies absorbed were the areas under the stress–strain curves below the strain of 0.3 and were calculated by numerical integration. The plateau strengths of the foams were determined differently for impact and static compression conditions. In the impact stress–strain curve of any syntactic foam, the average stress was nearly constant below the densification strain. The plateau strength was well defined and was obtained by averaging the stresses over the strains between 0 and 0.3. In the static compression stress–strain curve of any syntactic foam, the stress increased linearly in the elastic region and varied in a range in the plastic region between yielding and densification. The plateau strength was obtained by averaging the stresses over the strains between the yielding strain and 0.3. The yielding strains of Foams I, II, III and IV were estimated from Figure 5 to be roughly 0.05, 0.02, 0.05 and 0.03, respectively.

The four types of foams showed very different behavior. While Foams I and II had higher plateau strengths in impact than in static compression, Foams III and IV had lower plateau strengths in impact than in static compression. It seems that the different static and impact behavior is mainly due to the different volume fractions of Al in the syntactic foams. Foams I and II have low Al volume fractions (Table 2). In static compression, the deformation of the foams can change from compressive to shear mode at relative low strains as discussed in the previous section, leading to low plateau strengths. In impact, the high strain rate can hinder the rearrangement of the ceramic spheres required by shear deformation. The deformation of the foams under impact is more likely to remain compressive for a larger range of strain. As a consequence, the plateau strength is increased compared with that in static compression. In comparison, Foams III and IV have higher Al volume fractions (Table 2). More Al in the foams likely delays the transition from compressive deformation to shear deformation in static compression as discussed in the previous section. For foams with high Al volume fractions, the deformation process may be insensitive to strain rate. Furthermore, because Al is stronger than the porous ceramic spheres the mechanical response of the foams with high Al volume fractions may depend more on the Al network. The Al network can be seen as an Al foam, which normally exhibits higher strength in static compression than in impact [4,7]. As a consequence, the syntactic foams with more Al can show higher plateau strength in static compression than in impact. The deformation in the syntactic foams is a

***Table 4. Comparison between Al foam and Al matrix syntactic foam in energy absorption.***

| | | | | Syntactic | | | |
|---|---|---|---|---|---|---|---|
| **Foam** | | **Al** | | **I** | **II** | **III** | **IV** |
| Density (g/cm$^3$) | | 0.62 | 1.11 | 1.38 | 1.58 | 1.83 | 1.88 |
| Strength at 0.3 strain (MPa) | Static | | 34.5 | 41.7 | 33.3 | 55.6 | 51.4 |
| | Impact | 8.9 | | 62.3 | 62.1 | 40.6 | 44.1 |
| Specific energy, per volume (J/cm$^3$) | Static | | 5.7 | 12.1 | 9.8 | 15.4 | 14.7 |
| | Impact | 1.8 | | 18.4 | 18.2 | 12.0 | 13.1 |
| Specific energy, per mass (J/g) | Static | | 5.1 | 8.8 | 6.2 | 8.4 | 7.8 |
| | Impact | 2.9 | | 13.3 | 11.5 | 6.6 | 7.0 |

complex process lack of full understanding. The shape, size, and internal pore structure of the ceramic spheres and the infiltration defects can also affect the deformation mode. The deformation mechanisms behind the differences need further investigation.

As the elastic region of a syntactic foam is confined to within a relatively small strain, the specific energy absorbed by the foam at the densification strain is more or less proportional to the plateau strength. The specific energy absorbed, therefore, has the same trend as the plateau strength.

### Comparison with Al Foam

Table 4 compares the energy absorption properties of the Al matrix syntactic foams with those of the open cell Al foams fabricated by a pressure infiltration method [7]. Because the Al foams and the syntactic foams had a similar range of Al fractions, the Al foams had higher porosities, usually in the range of 0.6–0.8, and thus lower densities. Because of their higher porosities, the Al foams could undergo greater plastic deformation prior to full densification. However, the strengths of the Al foams were usually much lower than those of the syntactic foams at any strain. The pore sizes of the Al foams varied between 0.25–1.0 mm but their effects on the strengths were not significant. The Al foams did not show stress plateaus in the stress–strain curves in both static compression and impact. Instead, the stresses increased steadily with increasing strains. As a result, the amounts of energy absorbed by a unit volume of the Al foams were significantly lower than those of the syntactic foams, especially under the impact condition. The amounts of energy absorbed by a unit mass of the Al foams were also lower than those of the syntactic foams, although the differences were not as great. It is worth pointing out that the Al foams always had higher strengths in static compression than in impact at any particular strain. The different behavior of the two kinds of foams under different loading conditions is still not well understood. Nevertheless, the experimental results clearly showed that Al matrix syntactic foams have better energy absorption capacity in high stress circumstances.

## CONCLUSIONS

Aluminum matrix syntactic foams have been manufactured by infiltration casting using four types of porous ceramic spheres with diameters between 0.25 and 4 mm. The density

of the syntactic foams ranges from 1.38 to 1.88 g/cm$^3$ and the porosity ranges from 0.31 to 0.51. The syntactic foams showed different behavior in static compression and impact tests. In the static compression tests, they often cracked at relatively low strains and did not show well defined plateau strengths. In the impact tests, they had nearly constant plateau strengths and showed noticeable densification strains. Foams I and II had higher plateau strengths in impact than in static compression; Foams III and IV had lower plateau strengths in impact than in static compression. The plateau strength is largely determined by the volume fraction of Al in the foam, which has a dominant effect on the deformation mode in static compression and in impact. Foams I and II absorbed more energy under impact condition and less energy under static compression than Foams III and IV. Compared with the Al foams manufactured by a similar method, the syntactic foams had better energy absorption capacity, especially under impact conditions.

## ACKNOWLEDGMENTS

The authors would like to thank Dr. R. Birch for his assistance in conducting the impact tests and Mr. Z. H. Dun and Mr. Y. L. Huang for their assistance in preparing the syntactic foam samples. L. P. Zhang would like to thank the Daphne Jackson Trust for a Daphne Jackson Fellowship supported by the Leverhulme Trust.

## REFERENCES

1. Gibson, L.J. and Ashby, M.F. (1997). *Cellular Solids: Structure and Properties*. **2nd edn**, Cambridge: Cambridge University Press.
2. Banhart, J. and Eifert, H. (1997). *Metal Foams*. Verlag MIT Publishing, Bremen.
3. Davies, G.J. and Zhen, S. (1983). Metallic Foams – Their Production, Properties and Applications. *Journal of Materials Science*, **18**(7): 1899–1911.
4. Sun, D.X. and Zhao, Y.Y. (2003). Static and Dynamic Energy Absorption of Al Foams Produced by the Sintering and Dissolution Process. *Metallurgical and Materials Transactions B*, **34**(1): 69–74.
5. Banhart, J., Ashby, M.F. and Fleck, N.A. (1999). *Metal Foams and Porous Metal Structures*. Verlag MIT Publishing, Bremen.
6. Kiser, M., He, M.Y. and Zok, F.W. (1999). The Mechanical Response of Ceramic Microballoon Reinforced Aluminum Matrix Composites Under Compressive Loading, *Acta Materialia*, **47**(9): 2685–2694.
7. Zhao, Y.Y., Zhang, F.L. and Zhang, L.P. (2004). Impact Response of Aluminum and Aluminum Matrix Syntactic Foams. *Proceedings of International Conference on Planning, Design and Construction of Hardened and Protective Facilities*, Science and Technology Research Institute for Defence Malaysia, Kuala Lumpur, pp. 173–182,
8. Lide, D.R. (2004). *CRC Handbook of Chemistry and Physics*, **85th edn**, CRC Press, Boca Baton.
9. Hull, D. and Clyne, T.W. (1996). *An Introduction to Composite Materials*. **2nd edn**, Cambridge University Press, Cambridge, p. 63.